Scripta Materialia 146 (2018) 105–109

Contents lists available at ScienceDirect

Scripta Materialia

journal homepage: www.elsevier.com/locate/scriptamat

Regular article

Experimental evidence of liquid feeding during solidification of a steel

G. Agarwal [a,*], M. Amirthalingam [b], S.C. Moon [c], R.J. Dippenaar [c], I.M. Richardson [a], M.J.M. Hermans [a]

[a] Department of Materials Science and Engineering, Faculty of 3mE, Delft University of Technology, Mekelweg 2, 2628CD Delft, The Netherlands
[b] Department of Metallurgical and Materials Engineering, Indian Institute of Technology Madras, Chennai 600036, India
[c] School of Mechanical, Materials and Mechatronic Engineering, Faculty of Engineering and Information Sciences, University of Wollongong, Wollongong, Australia

ARTICLE INFO

Article history:
Received 16 September 2017
Received in revised form 26 October 2017
Accepted 2 November 2017
Available online 21 November 2017

Keywords:
Solidification
Steel
Solidification cracking
Hot tearing
In-situ

ABSTRACT

Sufficient liquid feeding under constrained solidification conditions like, those experienced in welding and casting, is vital to avoid solidification cracking. We present the results of unique *in-situ* experimental observations of liquid feeding in a solidifying steel melt pool. Liquid feeding was observed in the inter-cellular regions during the terminal stage of solidification. An average liquid flow speed of 450–500 μm s^{-1} was found. A pressure difference of the order of 10^4 Pa is calculated to cause the liquid flow. The rate of solidification shrinkage and the rate of deformation were found to be less than the rate of liquid feeding.

Some alloys are susceptible to cracking during solidification [1]. Solidification cracking during welding (similar to hot tearing during casting) has been studied for several decades [2–6]. Presently, it is accepted that a complex interplay between two fundamental factors; solidifying microstructure and restraint, leads to solidification cracking [7]. Upon cooling, a solidifying melt contracts due to both solidification shrinkage and thermal contraction. As the dendritic network becomes coherent, thermal strains are induced. If the remaining liquid is not able to compensate this deformation, cracking occurs. Eskin et al. [8] reviewed various hot tearing models for casting, including critical stress, strain and strain rate based criteria that lead to cracking. Nevertheless, a unified model involving the dominant physical factors is still lacking. This is partly due to the fact that solidification cracking occurs close to the solidus temperature (1673 K and above for low carbon steels) involving solid and liquid phases (mushy zone), limiting the scope of direct experimental based investigations. As a result, the various theories and models are rather difficult to verify.

Metallurgical factors that affect the cracking susceptibility include solidification temperature range, dendrite coherency, surface tension of the interdendritic liquid, viscosity, liquid feeding tendency, grain size and shape, solute segregation in the final stages of solidification *etc.* Liquid feeding is one of the most important factors that helps to avoid solidification cracking and likewise, is included in most of the models [1,9,10]. The early work of Feurer [9] was based on rate of feeding and rate of shrinkage effects on hot cracking phenomena. Cracking occurs if during solidification, the rate of feeding of the liquid in the inter-dendritic region is less than the rate of shrinkage of the solid being formed. The model proposed by Rappaz et al. [10] considered liquid feeding due to deformation of the coherent dendritic network and shrinkage. If the liquid feeding in the inter-dendritic region of the mushy zone is insufficient to compensate for the shrinkage and cumulative deformation of the mushy zone, the pressure drops below a certain cavitation pressure and voids form, grow and eventually coalesce to form a crack. Recently, Kou [1] proposed a model focussing on similar events occurring at grain boundary level.

Observing the solidification process in the mushy zone in welding conditions is difficult. In the past decade, high energy X-rays sources have facilitated the *in-situ* study of solidification behaviour in many metallic materials [11–14]. These studies are mostly focussed on Al-Cu, Sn-Pb, Al-Ni and other such systems with relatively low liquidus temperatures [15]. Studies in Fe-C systems are in general focussed on solid state phase transformations. Nagira et al. [15] observed *in-situ* deformation in semi-solid carbon steel. They studied the deformation mechanism under direct shear of the steel with a globular morphology and solid fraction between 55–65 %. Several other techniques like directional solidification (Bridgman technique [16]), high speed camera observations of the weld pool solidification [17] *etc.* are also frequently used to study solidification phenomena. None of

* Corresponding author.
E-mail address: g.agarwal@tudelft.nl (G. Agarwal).

https://doi.org/10.1016/j.scriptamat.2017.11.003
1359-6462/

the studies, however, have reported direct observation of liquid flow during the terminal stages of solidification.

In this work, solidification of a dual phase steel was observed *in-situ* using high temperature laser scanning confocal microscopy. This technique is frequently used to study *in-situ* solidification events like peritectic transformations and solid-state transformations, details of which can be found in the literature [18,19]. In the present work, a circular melt pool was formed at the centre of a thin circular disk specimen while the outer rim remained solid. The solid outer rim acted as a restraint to the solidifying melt pool, thus allowing the simulation of welding conditions. During the terminal stages of solidification, liquid feeding was observed in inter-cellular regions. The feeding rate in these regions is calculated and subsequently the pressure that causes liquid feeding is estimated.

A commercial dual phase steel sheet with a composition, C 0.15, Mn 2.3, Cr 0.56, Si 0.1, Al 0.03, P 0.01 (all in wt.%) was examined in this study. Circular disk specimens with a diameter of 10 mm and a thickness between 200 μm–250 μm were prepared using electro-discharge machining. Each specimen was placed in an alumina crucible. To minimise direct contact with the alumina crucible, the sample was held by ceramic protrusions at the circumference of the crucible. The crucible in turn was held in a platinum holder. A B-type thermocouple wire was welded to the platinum holder. Specimens were placed at the upper focal point of a gold plated ellipsoidal cavity in an infra-red furnace beneath a quartz view port under an ultra-high purity inert gas atmosphere, >99.9999% Ar. A 1.5 kW halogen lamp located at the lower focal point in the cavity heats the specimen by radiation. The power input to the halogen lamp is controlled by an Omron ES100P digital PID controller, which in turn was connected to the thermocouple at the crucible holder for a feedback signal. The temperature measured by the thermocouple incorporated in the crucible holder was recorded while simultaneously, optical images were recorded at a rate of 30 frames per second. A stable melt pool with a diameter between 3–3.5 mm was obtained at the centre of the specimen while the outer rim remained solid. A cooling rate of 5 K min^{-1} was employed until 1623 K. To obtain an approximation of the actual temperature in the liquid pool, experiments with pure iron samples were conducted and a difference of 210 K was found between the thermocouple reading and melting point of iron (taken as 1811 K).

Fig. 1 shows the solidification sequence of the steel. A stable melt pool of diameter 3.1 mm was created before the cooling cycle started, as seen in Fig. 1 (a). Due to the slow cooling rate, the solidification front was initially observed to remain planar (Fig. 1 (b)). On further cooling, the interface morphology changed from planar to cellular growth as seen in Fig. 1 (c). On a macro scale, the solid/liquid interface was observed to propagate in a concentric manner throughout the solidification process. Concentric propagation of the interface was tracked using automatic video processing software for *in-situ* interface tracking [20]. The radius of curvature of the interface can be used to calculate the fraction of solid and liquid at any time. Fig. 1 (d) shows the terminal stage of the solidification during which the liquid feeding was observed in the inter-cellular regions. The fraction of liquid remaining was ≈ 1.2% when compared to the original melt pool size. Two regions where liquid feeding was observed are marked in Fig. 1 (d) and further shown in Figs. 2 and 3 respectively. The liquid source for the feeding is the liquid remaining during the final stage of solidification in the centre. The process was dynamic and occurred in a matter of a few seconds. For better visualisation of the liquid flow, the reader can refer to the video file included as a supplement in the online version of this article. Fig. 2 shows the images from region 1 with F-*n* indicating the frame numbers. Time difference between successive frames is 33.33 ms. In order to determine the extent of liquid flow, reference grey scale image, Fig. 2 (a), was

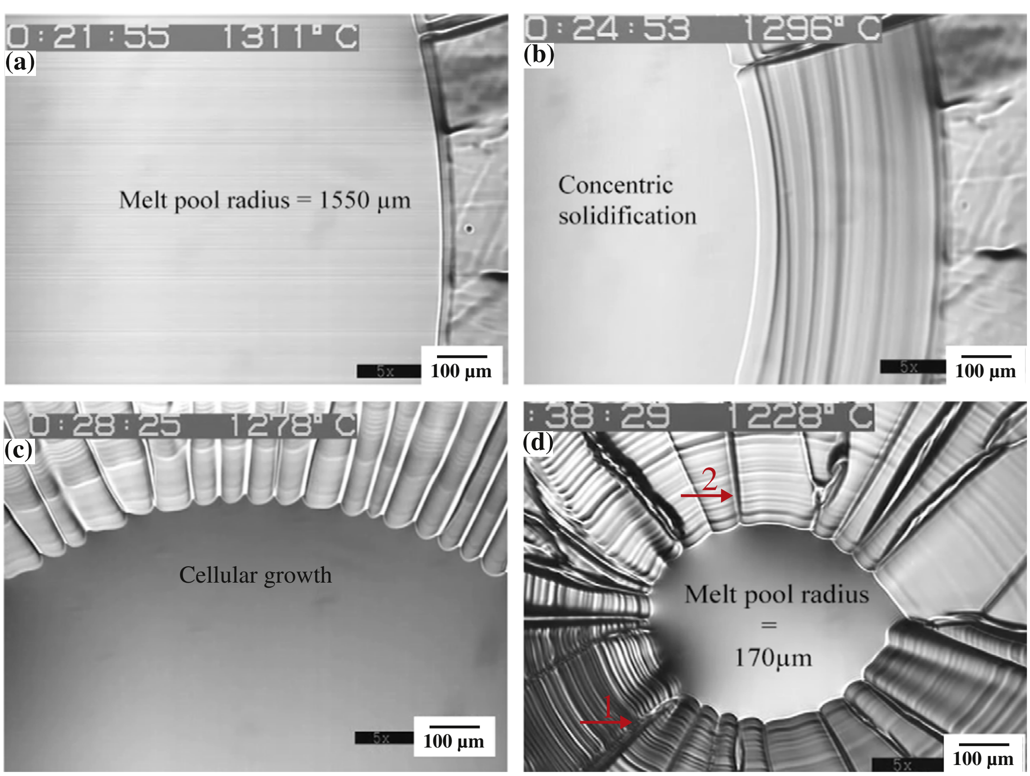

Fig. 1. Solidification images. (a) A stable melt pool of radius 1550 μm is formed to begin with. Afterwards a constant cooling rate of 5 K min^{-1} is applied, (b) solidification progresses in a concentric manner, (c) planar growth changes to cellular, (d) melt pool of radius 170 μm when liquid feeding in the inter-cellular regions was observed. Temperature indicated in images (a–d) is measured at the periphery of the platinum holder. Based on calibration the actual temperature is ~ 210 K higher.